Organic & Biomolecular Chemistry

Accepted Manuscript

ROYAL SOCIETY OF CHEMISTRY

www.rsc.org/obc

Organic & Biomolecular Chemistry

Dynamic Article Links ►

Cite this: DOI: 10.1039/c0xx00000x

PAPER

www.rsc.org/xxxxxx

Characterisation of radicals formed by the triazine 1,4-dioxide hypoxia-activated prodrug, SN30000.

Robert F. Anderson,*[a, b] Pooja Yadav,[a] Deepa Patel,[b] Jóhannes Reynisson,[b] Smitha R. Tipparaju,[a] Christopher P. Guise,[a] Adam V. Patterson,[a] William, A. Denny,[a] Andrej Maroz,[b] Sujata S. Shinde[a] and Michael P. Hay.[a]

Received (in XXX, XXX) Xth XXXXXXXXX 20XX, Accepted Xth XXXXXXXXX 20XX
DOI: 10.1039/b000000x

The radical species underlying the activity of the bioreductive anticancer prodrug, SN30000**,** have been identified by electron paramagnetic resonance and pulse radiolysis techniques. Spin-trapping experiments indicate both an aryl-type radical and an oxidising radical, trapped as a carbon-centred radical, are formed from the protonated radical anion of SN30000. The carbon-centred radical, produced upon the one-electron oxidation of the 2-electron reduced metabolite of SN30000, oxidises 2-deoxyribose, a model for the site of damage on DNA which leads to double strand breaks. Calculations using density functional theory support the assignments made.

Introduction

Hypoxic cells represent an important challenge for cancer therapy as hypoxia in tumours results in resistance to chemotherapy through increased expression of multi-drug resistance proteins,[1] reduced cell cycling under severe hypoxia[2] and limited penetration of blood-borne anticancer drugs into hypoxic tissue distant from functional blood vessels.[3] In addition, hypoxic cells are markedly resistant to radiotherapy[4] compared to oxic cells where oxygen enhances radiation-induced radicals on DNA to cytotoxic strand breaks.[5] However, severe hypoxia in tumours relative to normal, well-oxygenated tissue, also offers an opportunity in developing hypoxia-selective cytotoxins which are able to target this physiological feature of tumours.[6] An approach for exploiting tumor hypoxia is to employ relatively inert drugs which undergo selective one-electron reduction as hypoxia-activated prodrugs (HAP) to release cytotoxins.[6] This principle is the basis for the clinical evaluation of the nitroimidazole prodrug TH-302, which acts primarily by hypoxia-selective release of a potent DNA cross-linking metabolite.[7,8] The benzotriazine 1,4-dioxide (BTO) class of drugs, of which tirapazamine (TPZ, 3-amino-1,2,4-benzotriazine 1,4-dioxide), is the most extensively investigated HAP, undergo oxygen-inhibited reduction[9] to an intermediate which breaks down to form reactive radicals, including benzotriazinyl radicals,[10,11] as well as possibly aryl radicals,[12] that induce oxidative damage on DNA similar to •OH radical attack.[13-15] Although TPZ showed promising efficacy in early clinical trials[16,17] this did not extend to increased survival in combination with cisplatin and radiotherapy in a multi-centered phase III clinical trial for advanced head and neck cancers.[18] Failure at phase III has been ascribed to both non-selection for patients with hypoxic tumours[19] and sub-optimal radiotherapy given in some of the centres.[20] It is also possible that metabolic consumption of TPZ during its diffusion to the most deeply hypoxic cells prevents a sufficient concentration in such cells,[21] and that the radicals produced, following one-electron reduction of TPZ, are not optimal in oxidising power or in sufficient quantity to cause enough wide-spread damage to be expressed as a therapeutic effect.

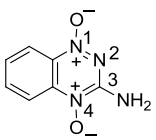

TPZ

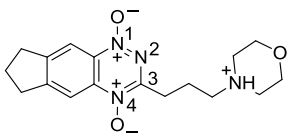

SN30000, **1**

To address the drug diffusion concerns, the TPZ analogue SN30000, **1**, (3-[3-(4-morpholinyl)propyl]-7,8-dihydro-6H-indeno [5,6-e][1,2,4] triazine 1,4-dioxide) has been identified to possess a higher diffusion coefficient and improved extravascular transport than TPZ by using both multicellular layer cultures and a spatially-resolved pharmacokinetic/ pharmacodynamics model.[22] Previous work has shown that the design feature of replacing the 3-amine substituent of TPZ with 3-alkyl can result in the production of the more powerful benzodiazinyl oxidizing radical,[14] however the radical chemistry of SN30000 is unknown. On the basis of higher hypoxic selectivity and potency of SN30000 compared to TPZ in tissue culture and improved activity in xenograft models,[22] it is undergoing preclinical development. In this paper we examine the dynamic radical chemistry of SN30000 to better understand the initial events that underpin its hypoxia-selective

cytotoxicity, as a pointer to improving this class of HAP. The mechanistic framework for this study is presented in Scheme 1.

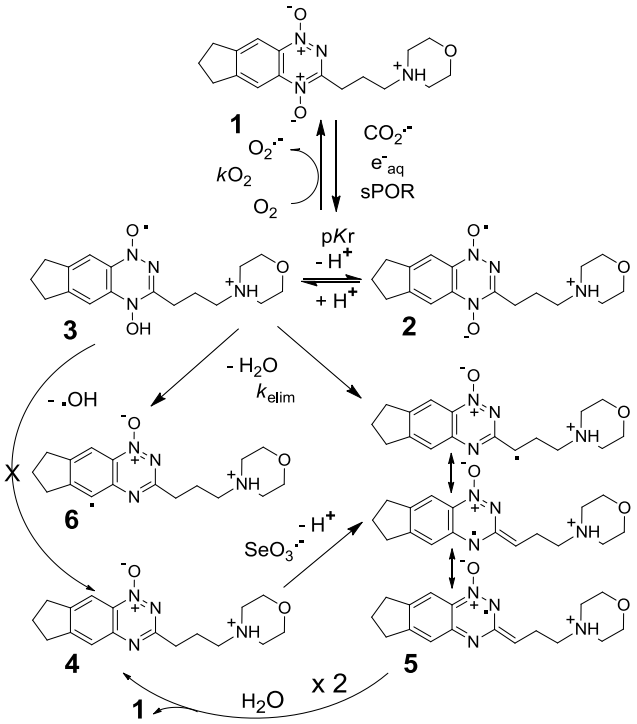

Scheme 1. Pathways for the formation, and reactions of radical species formed after the one-electron reduction of SN30000, **1**.

Results and discussion

Pulse radiolysis studies

The one-electron reduction potential value, $E(1)$, of SN30000, **1**, and its 1-oxide, 2-electron-reduced metabolite, **4**, Scheme 1, were determined by establishing redox equilibria against methyl viologen and triquat as reference standards following reduction by the e^-_{aq}. The $E(1)$ value of **1** of -401 ± 8 mV is 55 mV higher than TPZ, which possesses the strongly electron donating 3-NH_2 group rather than the weaker 3-alkyl substitution. The $E(1)$ value of 4 (-471 ± 8 mV) is some 100 mV higher than the 1-oxide metabolite of TPZ (-568 mV)[9] and is in the region for further efficient bioreduction. The radical anion spectrum, **2**/**3**, was produced upon reaction of the $CO_2^{\bullet-}$ radical with **1**, Fig.1. The spectrum in the visible region varied in absorption intensity with pH and this was utilised to determine the pK of the radical anion as pKr = 5.48 ± 0.26, Fig. 1, Insert. The decay of the radical anion followed 1st-order kinetics, exhibiting a plateau in rate constant at low pH ($k$max = 776 ± 30 s^{-1}) and decreasing rate constants with increasing pH. At near neutral pH the radical anion, **2**/**3**, decayed with mixed order kinetics and transients obtained at different radiation doses were analysed as previously described using plots of the inverse of the first half-life, 1/t0.5 versus, [**2**/**3**] to separate out the slow 1st-order component from the

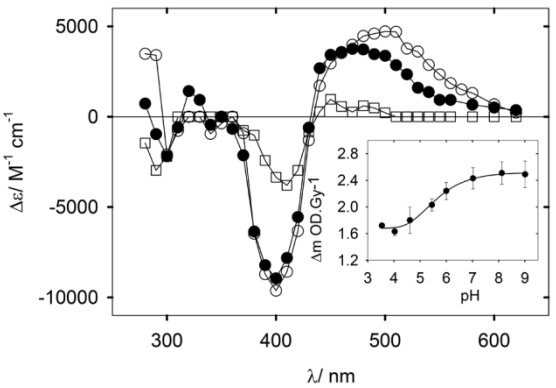

Fig. 1. Absorption difference spectra of radicals, relative to parent compound, at pH 9.0 (o), pH 5.1 (●) at 20 μs and pH 5.1 (□) 4 ms following pulse radiolysis (2.5 Gy in 200 ns) of **1** (0.15 mM) in N_2O-saturated solutions containing sodium formate (0.1 M) containing phosphate buffers (20 mM). Insert: Dependence of 480 nm absorption, measured at 20 μs, on pH.

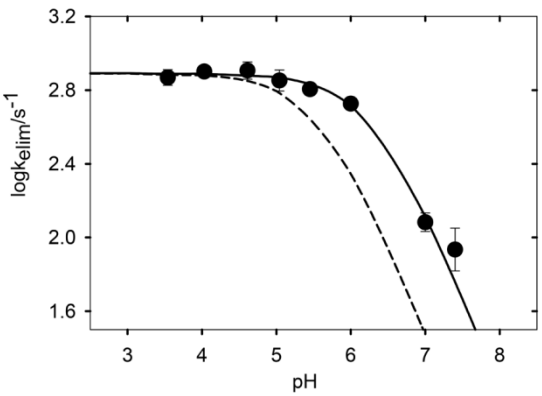

Fig 2 Dependence of the 1st-order rate constant for the decay of radical anion **2**/**3** on pH. Dashed line represents predicted dependency for a radical pKr of 5.48 (see text); Solid line is drawn for a radical pKr of 6.3.

bimolecular decay of the radical anion.[10] At pH 7, k = 125 ± 15 s^{-1}. The dependence of the 1st-order decay process on pH, is ascribed to a unimolecular loss of water, k_{elim}, from the protonated radical anion, similar to related BTO compounds. However, unlike for TPZ and close analogues, k_{elim} does not follow the expected dependence of $k_{elim} = (k_{max} \times [H^+])/([H^+] + Kr)$, exhibiting greater rate constants than predicted, Fig. 2. The data points fit the expression for a pKr of 6.3, which may well indicate the influence of the protonated morpholine side chain of the radical anion, which is expected to be of slightly lower pK than for the unreduced compound, of pK 7.1. The pseudo 1st-order kinetics for the back oxidation of the radical anion by molecular oxygen, in competition to its k_{elim}, was determined from the decay of the transients at 500 nm in solutions saturated with mixtures of O_2 and N_2, Fig. 3. The 2nd-order rate constant determined from the plot, k_{O2} = 3.33 ± 0.03 × 10^6 M^{-1} s^{-1}, is as predicted for the dependency of k_{O2} on $E(1)$ for a wide range of nitrobenzenes, nitroheterocycles and BTO compounds.[11,23]

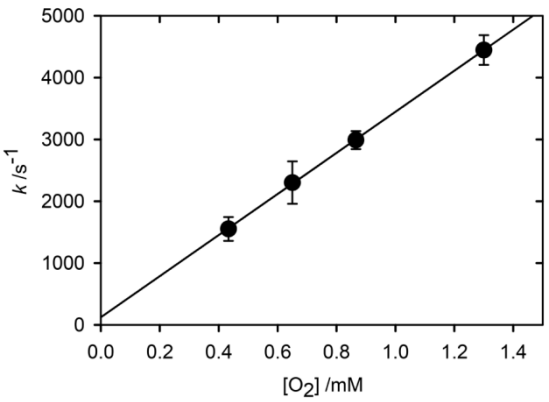

Fig. 3. Dependence of the 1st-order rate constant for the decay of radical anion **2**/**3** on the concentration of O_2.

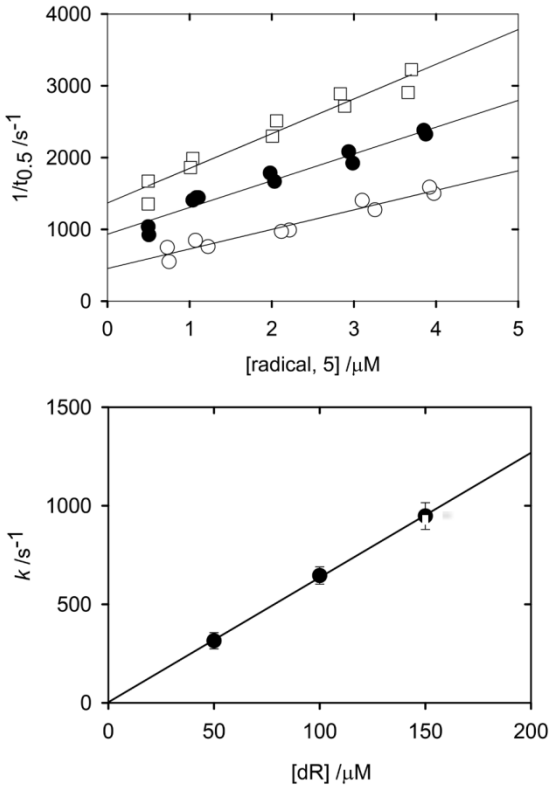

Fig. 4. Upper panel: Plot of the dependence of the reciprocal of the first half-life of **5** on the initial radical concentration, formed with increasing radiation dose, in the presence of; ○ 50 μM, ● 100 μM and □ 150 μM dR. Lower panel: Plot of pseudo 1st-order rate constants, derived from the intercepts above, against the concentration of 2-deoxyribose (dR).

The intercept of the plot in Fig. 3, 120 ± 23 s^{-1}, is the rate constant for a competitive 1st-order reaction, independent of O_2 concentration, which agrees with k_{elim}, determined above. Loss of water from the protonated anion, **3**, can be envisaged to result in the formation of either, or both, radicals **5** and **6**. The oxidizing benzodiazinyl radical, BDZ, **5**, has resonance forms spread over the heterocylic Ns, in an analogous manner to BTO compounds, which form a benzotriazinyl radical, BTZ.[24] One-electron oxidation of the two-electron reduced metabolite, **4** to form the benzodiazinyl radical[5] was carried out and a redox equilibriu m was established between it and 1,4-dimethoxybenzene to determine the radical one-electron reduction potential, $E(1)R$ of 1.35 ± 0.02 V. Reaction between radical **5** and 2-deoxyribose (dR), a model for the site of DNA strand breaks) was studied using the same method as above to separate out the pseudo 1st-order reaction between each of three concentrations of dR (50–150 μM) and the 2nd-order, radical-radical decay, for a range of radiation doses (1.5–15 Gy), Fig. 4. Plotting the rate constants derived from the intercepts of the plots against [dR], Fig. 4, yields the 2nd-order rate constant, $k_{oxid} = 6.33 \pm 0.17 \times 10^6$ M^{-1} s^{-1}, between **5** and dR. This value conforms to the same relationship between $E(1)R$ and k_{oxid} for the BTO compounds[15] and is greater than for the reaction between the BTZ radical of TPZ and dR.

EPR spectra of radical intermediates

EPR studies were undertaken to gain insight into possible structural features of the radical intermediates using spin traps. One-electron reduction of **1** by NADPH cytochrome P450 oxidoreductase (sPOR) was carried out anaerobically at 310 K *in situ* in an EPR spectrometer. The EPR spectrum of radicals trapped by PBN is presented in Fig. 5, which exhibits a triplet of

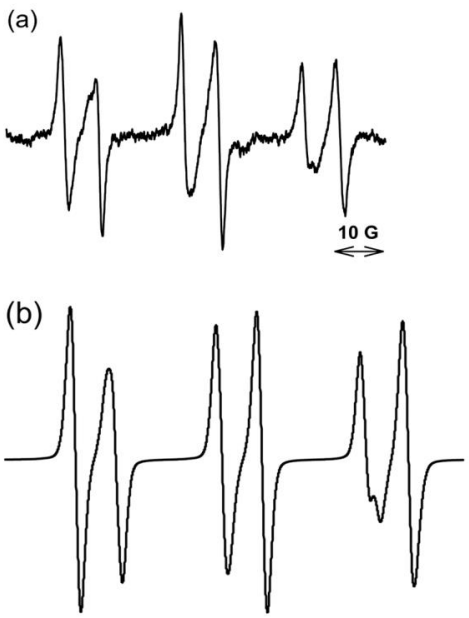

Fig. 5. (a) EPR spectra of radicals obtained upon reduction of SN30000 (12 mM) by sPOR protein (6 ng.mL^{-1}) in solutions at 310 K containing DETAPAC (100 μM), SOD (300 units.mL^{-1}), catalase (1500 units.mL^{-1}), glucose-6-phosphate-dehydrogenase (13 units.mL^{-1}), glucose-6-phosphate (10 mM), and NADPH (1 mM) at pH 7 in presence of PBN (50 mM) and SN30000 ; (b) simulated spectrum (NIH WinSim) of (i) PBN-aryl (0.57) and (ii) PBN-C centred species (0.43), r = 0.962.

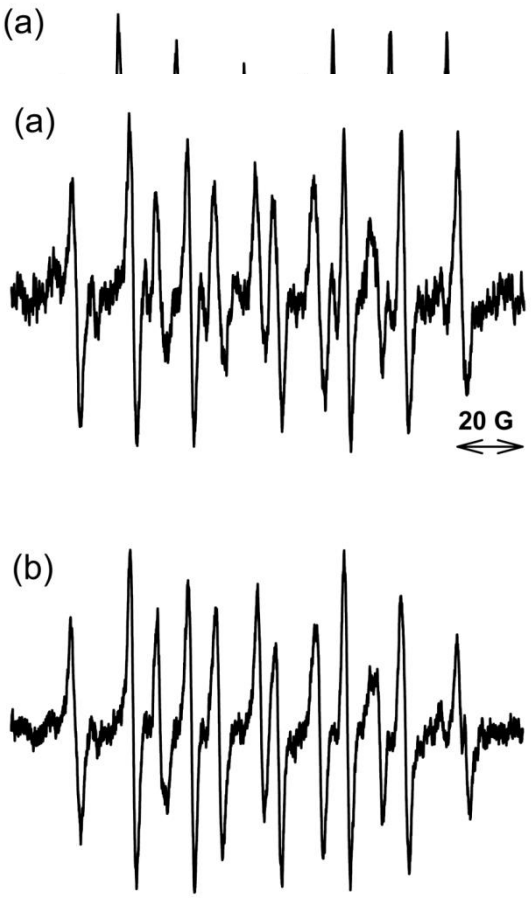

Fig. 6. (a) EPR spectra of radicals obtained upon reduction of SN30000 (12 mM) by sPOR protein (6 ng/ml) in solutions at 310 K containing DETAPAC (100 μM), SOD (300 units.mL^{-1}), catalase (1500 units.mL^{-1}), glucose-6-phosphate-dehydrogenase (13 units.mL^{-1}), glucose-6-phosphate (10 mM), and NADPH (1 mM) at pH 7 in presence of DEPMPO (25 mM) ; (b) with DMSO (2 M) added.

doublets displaying wide splitting. This spectrum could be simulated by combining two species in the ratio 0.4:0.6 with hyperfine coupling constants (HFC) of (i) aH 4.2 G aN 16.0 G, and (ii) aH 3.44 G aN 16.2 G, Fig. 5. The HFC of (i) match those of a phenyl-type radical[25,26] and (ii) are similar to a carbon-centred radical such as the ethyl radical.[27] No EPR evidence was obtained for spin trapping of the ·OH radical, which has been suggested to be formed following the one-electron reduction of BTO compounds.[13,14,28-30] Further experiments were carried out using DEPMPO as the spin trap, as the pyrroline N-oxides trap both oxygen-centred and carbon-centred radicals, but are susceptible to oxidation through spin inversion,[31] Fig. 6. The initial recorded spectrum exhibited both a 12-line spectrum, with HFC of aH 22.1 G aN 15.2 G aP 48.8 G and an 8-line DEMPO-OH spectrum (not shown), which gradually disappeared over an hour time period to leave the 12-line spectrum presented in Fig. 6. The 12-line spectrum is general for a carbon-centred radical,[32] which is likely to be the favoured spin-trappable form of the BDZ radical by DEMPO. The same pattern of EPR spectra formation and decay were observed on adding a high concentration of DMSO (2M). DMSO is an effective scavenger of ·OH radicals, releasing methyl radicals[33] which would be trapped to give a different spectrum.[34] As no changes in the EPR spectrum occurred, it can be concluded that the DEMPO-OH spectrum observed on the short time scale arises from radical oxidation of the spin trap and not from addition of the ·OH radical.

DNA double strand breaks

The relative activities of SN30000 and TPZ to cause DNA

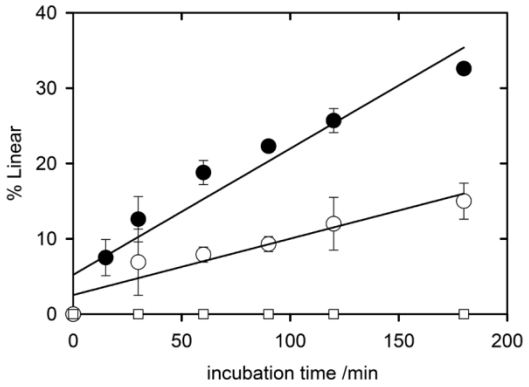

Fig. 7. Production of linear DNA upon anaerobic incubation of plasmid pCMV.sp (50 ng.μL^{-1}), NADPH (1 mM), rat liver POR protein (20 μL.mL^{-1}) in Tris buffer (5 mM, pH 7.4) at 37°C, □; TPZ (0.2 mM) added, ○; SN30000 (0.2 mM) added, ●.

double strand breaks (DSB) upon reduction were tested using the plasmid DNA system,[35] with reduction supported by rat liver microsomes containing NADPH cytochrome P450 reductase (POR), a known activating enzyme of TPZ.[36] Unrepaired DSB are a lethal lesion in cells.[37,38] The proportion of DSB were determined as linear DNA bands at serial time points via gel electrophoresis and plotted as the percentage linear DNA against the time of incubation with POR, Fig. 7. Both SN30000 and TPZ are active under anaerobic conditions causing DSB, with SN30000 effecting *ca*. twice as much as TPZ over the 3 hour incubation period. No linear DNA bands were formed when the compounds were tested under aerobic conditions (data not shown). The greater DSB activity of SN30000 than TPZ most likely arises from a combination of it possessing a more positive $E(1)$ value (greater rate of metabolism) and its BDZ radical having a higher reduction potential than the BTZ radical formed by TPZ, which has been shown above to react faster with dR, the site of DNA strand breakage. The formation of aryl radicals is also a common link in the reactivity of the two bioreductive compounds. Aryl radicals are strong oxidants capable of inducing widespread cellular damage, including DNA strand breaks.[39,40]

DFT calculations

Calculations of the relative changes in free energy for the 4-oxide protonated radical anion, **3**, to undergo the three elimination pathways in Scheme 1 were performed: (i) **3** → **4** (1-oxide plus ·OH radical elimination), (ii) **3** → **5** (H_2O plus BDZ radical, and (iii) **3** → **6** (H_2O plus aryl radical), and are presented in Table 1.

Also included are data for elimination pathways to produce both the ·OH radical and the aryl radical from the protonated 1-oxide radical anion. These results indicate that elimination of water from the radical anion protonated at the 4-oxide position is more favourable leading eventually to the 1-oxide metabolite, **4**, in agreement with pharmacokinetic studies.[22] Of the three possible elimination pathways investigated, formation of the BDZ radical, **5**, is more exothermic than formation of the aryl radical, **6**, while production of the ·OH radical and the 1-oxide, **4**, is slightly endothermic.

Radical anion		Proton affinity	·OH release	-H_2O (Aryl)	-H_2O (BDZ)
proton on 4-oxide	Gas H_2O	-325.1 -281.3	+3.5 +1.4	+1.1 -2.9	-27.2 -30.1
proton on 1-oxide	Gas H_2O	-324.7 -280.6	+14.4 +11.7	+12.3 +7.7	N/A N/A

Table 1. DFT derived values for the change in energy (kcal.mol^{-1}) for the protonation affinity (PA) and subsequent formation of radicals from the 1-oxide and 4-oxide protonated radical anions formed upon the one-electron reduction of **1**. Upper values are for the gas phase; lower values are upon water solvation, as described in the text.

Conclusions

SN30000 undergoes one-electron reduction to form an oxygen-sensitive radical anion which is unstable and forms oxidising radicals. Both an aryl-type radical, and most likely the carbon-centred form of the BDZ radical, are able to be spin-trapped. Such radicals are strong oxidising species, making them candidate radicals underlying the known cytotoxicity of this class of bioreductive compounds in causing DNA double strand breaks.

Experimental section

All reagents used were of analytical grade. Sodium formate, sodium hydroxide, perchloric acid and phosphate buffers were obtained from Merck and potassium thiocyanate from Reidel-de Haën. All other reagents were obtained from Sigma-Aldrich. All solutions were prepared in water purified by the Milli-Q system. Solution pH values were adjusted using phosphate salts (5 mM) and either NaOH or $HClO_4$. TPZ,[41] SN30000, **1** and its 1-oxide derivative, **4**, were prepared as previously described.[22] Pulse radiolysis and time-resolved spectrophotometry experiments were carried out using the University of Auckland's 4 MeV linear accelerator of variable pulse length (200 ns to 1.5 μs), to deliver absorbed dose of 2.5 Gy for spectral studies and up to 10 Gy for kinetic studies at room temperature (295 ± 1 K).[42]

Preparation of recombinant human NADPH:cytochrome P450 oxidoreductase (sPOR)

Soluble NADPH:cytochrome P450 reductase (sPOR)[43] was cloned in plasmid pET28a+ and expressed with an N-terminal His-tag in BL21 (DE3) *E. Coli*. Exponentially growing cultures (LB broth containing 50 μg.mL^{-1} kanamycin, 1 mg.mL^{-1} riboflavin) were induced with IPTG (0.5 mM) and incubated (RT, 24 hr). Bacteria were harvested, resuspended in lysis buffer (5 mM imidazole, 500 mM NaCl, 20 mM Tris.HCL pH 7.9 plus protease inhibitor cocktail [Sigma Aldrich]), sonicated and clarified by centrifugation (9000g, 277 K, 1 hr). Supernatant was filtered incrementally (1.2, 0.80, 0.45, 0.20 microns) prior to nickel column purification (AKTAprime chromatography; GE healthcare). Protein was concentrated (50,000 MW cut off; Amicon) prior to gel filtration (AKTAprime chromatography). Protein was re-concentrated with subsequent addition of 100 μM flavin mononucleotide and flavin adenine dinucleotide and diluted 1:1 in pure glycerol. Purity of sPOR protein was confirmed by SDS-PAGE with Coomassie blue staining or immunodetection as described.[44] Rat liver microsomes, at a concentration of 16 mg.mL^{-1} protein, were also prepared as a source of POR.[45] POR activity was determined by spectrophotometric assay as the cyanide-resistant reduction of cytochrome c in the presence of NADPH, as described previously.[46]

Radiation chemistry

The radiolysis of water produces three well-characterized reactive radical species used to initiate radical reactions, as well as molecular products (μM per absorbed dose of 1 Gy (J Kg^{-1}) given in parenthesis).

$$H_2O \text{ ^^^^}\rightarrow e_{aq}^-(0.28) + \cdot OH(0.28) + H\cdot(0.055) + H_2(0.04) + H_2O_2(0.07) + H_3O^+(0.28)$$

One electron reduction of **1** and **4** were carried out by (i) the e_{aq}^-, while at the same time scavenging the oxidizing radicals with 2-methylpropan-2-ol to form an inert radical, (ii) electron transfer from the $CO_2^{\cdot-}$ species (E $CO_2/CO_2^{\cdot-}$) = -1.90 V[47]) in N_2O-saturated solutions (to quantitatively convert the e_{aq}^- to ·OH radicals) containing 0.1 M sodium formate, to convert the ·OH radicals and H-atoms into $CO_2^{\cdot-}$.

$$e_{aq}^- + A / B \rightarrow A^{\cdot-} / B^{\cdot-}$$

$$\cdot OH(H\cdot) + (CH_3)_3COH \rightarrow \cdot CH_2(CH_3)_2COH + H_2O(H_2)$$

$$N_2O + e_{aq}^- \rightarrow \cdot OH + OH^- + N_2$$

$$\cdot OH(H\cdot) + HCOO^- \rightarrow H_2O(H_2) + CO_2^{\cdot-}$$

$$CO_2^{\cdot-} + A / B \rightarrow A^{\cdot-} / B^{\cdot-} + CO_2$$

One-electron oxidation of the benzotriazine 1-oxide, **4**, (B) was carried out by reaction with the selenite radical ($SeO_3^{\cdot-}$) produced on scavenging the e_{aq}^- by sodium selenate (50 mM) in deaerated solutions containing 2-methylpropan-2-ol (0.2 M) to scavenge the ·OH radicals.

$e_{aq}^- + SeO_4^{2-} + H_2O \rightarrow SeO_3^{\bullet -} + 2OH^-$

$SeO_3^{\bullet -} + B \rightarrow B^\bullet + H^+ + SeO_3^{2-}$

One-electron reduction potentials

The one-electron reduction potentials of SN30000 and its 1-oxide metabolite, E(**1**/**2**) and E(**4**/**4**$^{\bullet -}$) vs. NHE, were determined at pH 7.0 (2.5 mM phosphate buffer) by observing the establishment of redox equilibria between three mixtures of the one-electron reduced compounds and the reference compounds methylviologen (E($MV^{2+}/MV^{+\bullet}$) = -447 ± 7 mV) and triquat (E($TQ^{2+}/TQ^{+\bullet}$) = -548 ± 7 mV) respectively. The equilibrium constants, Ke, were determined from observations of the absorbances at 600 nm and 385 nm respectively from which ΔE values were calculated using the Nernst equation, as described in the literature.[48] Similarly, the one-electron reduction potential of the benzodiazinyl radical, E(**5**, H^+/**4**), was determined by measuring the redox equilibrium formed between three mixtures of the oxidised benzotriazine 1-oxide and the reference compound 1,2-dimethoxybenzene (E($DMB^{+\bullet}$/DMB) = 1.30 ± 0.1 V[49]).

$$MV^{+\bullet}/TQ^{+\bullet} + \mathbf{1/4} \overset{Ke}{\rightleftharpoons} MV^{2+}/TQ^{2+} + \mathbf{2/4}^{\bullet -}$$

$$DMB^{+\bullet} + B \overset{Ke}{\rightleftharpoons} B^\bullet + H^+ + DMB$$

The radical pKa value (pKr), for **3**/**2** was derived by non-linear least-squares fit to a sigmoidal function, using Origin software.

Electron Paramagnetic Resonance (EPR) experiments

EPR experiments were carried out within a TE011 cavity on a JOEL (JES-FA-200) EPR spectrometer equipped with a variable temperature controller and operated at 9.1 GHz and 100 kHz field modulation. Human sPOR protein was used to reduce SN30000 under anaerobic conditions at 310 K in the presence of the spin traps, *N*-*tert*-butylphenylnitrone (PBN) and 5-(diethoxy-phosphoryl)-5-methyl-1-pyrroline (DEPMPO), a NADPH regenerating system and both enzymatic and chemical scavengers of possible confounding redox active species.

DFT calculations

The geometry optimisation and energy calculations were performed with Gaussian 09 software suite using unrestricted DFT.[50] The non-local B3LYP functional hybrid method was employed[51-53] and the standard 6-31+G(d, p)[54,55] basis set was used for the geometry optimisation and frequency analysis. The zero-point vibrational energies (ZPE) were scaled according to Wong (0.9804).[56] In all cases, the normal modes revealed no imaginary frequencies indicating that they represent minima on the potential energy surface. The subsequent energy calculations were performed with the larger 6-311+G(2df, p) basis set. All of the structural optimisation and energy calculations were carried out with a water simulation based on the polarised continuum model (IEFPCM).[57] The morpholine moiety is protonated on the distal nitrogen for the solvent simulations. The reaction steps were calculated by subtracting the ZPE corrected energies of the reactants from the products. All the energies are given in Table S1 in the ESI.

DNA strand breaks

DNA double strand breaks were measured using the plasmid pCMV.SPORT-βgal (7854 bp) obtained from Life Technologies. The different forms of the plasmid: supercoiled, circular (relaxed, single-strand break) and linear (double strand break) were separated on agrose gels (1%) by electrophoresis,[35] stained with ethidium bromide and their percentages quantified from their digital images, allowing for a 1.3 enhanced staining of the supercoiled form. Anaerobic reductions of SN30000 and TPZ, dissolved in Tris buffer containing the plasmid and the lysate from rat liver microsomes, were carried out in glass vessels continually purged with humidified N_2 gas at 310 K, to which was added NADPH to initiate the reactions. Serial samples from triplicate experiments were withdrawn and examined for drug-related DNA strand breaks.

Acknowledgements

This work was supported by Grants 07/243 and 11/323 from the Health Research Council of New Zealand.

Notes and references

[a] *Auckland Cancer Society Research Centre, Faculty of Medical and Health Sciences, University of Auckland, Private Bag 92019, Auckland 1142, New Zealand. Fax: +64 9 3737502; Tel: +64 9 9238315; E-mail: r.anderson@auckland.ac.nz*

[b] *School of Chemical Sciences, Faculty of Science, University of Auckland, Private Bag 92019, Auckland 1142, New Zealand.*

† Electronic Supplementary Information (ESI) available: [EPR control experiments, full reference 50 and DFT calculated energies]. See DOI: 10.1039/b000000x/

1 K. M. Comerford, T. J. Wallace, J. Karhausen, N. A. Louis, M. C. Montalto and S. P. Colgan, *Cancer Res.*, 2002, **62**, 3387-3394.
2. I. M. Pires, Z. Bencokova, M. Milani, L. K. Folkes, J.-L. Li, M. R. L. Stratford, A. L. Harris and E. M. Hammond, *Cancer Res.*, 2010, **70**, 925-935.
3. A. I. Minchinton and I. F. Tannock, Nature Rev. *Cancer*, 2006, **6**, 583-592.
4. L. H. Gray, A. D. Conger, M. Ebert, S. Hornsey and O. C. A. Scott, *Br. J. Radiol.*, 1953, **26**, 638-648.
5. P. Wardman, *Radiat. Phys. Chem*., 1987, **30**, 423-432.
6. W. R. Wilson and M. P. Hay, Nat. Rev. *Cancer*, 2011, **11**, 393-410.
7. K. N. Ganjoo, L. D. Cranmer, J. E. Butrynski, D. Rushing, D. Adkins, S. H. Okuno, G. Lorente, S. Kroll, V. K. Langmuir and S. P. Chawla, *Oncology*, 2011, **80**, 50-56.
8. G. J. Weiss, J. R. Infante, E. G. Chiorean, M. J. Borad, J. C. Bendell, J. R. Molina, R. Tibes, R. K. Ramanathan, K. Lewandowski, S. F. Jones, M. E. Lacouture, V. K. Langmuir, H. Lee, S. Kroll and H. A. I. Burris, *Clin. Cancer Res.*, 2011, **17**, 2997-3004.
9. K. Laderoute, P. Wardman and A. M. Rauth, Biochem. Pharmacol., 1988, 37, 1487-1495.

10. R. F. Anderson, S. S. Shinde, M. P. Hay, S. A. Gamage and W. A. Denny, *J. Am. Chem. Soc.*, 2003, **125**, 748-756.
11. R. F. Anderson, S. S. Shinde, M. P. Hay, S. A. Gamage and W. A. Denny, *Org. Biomol. Chem*., 2005, **3**, 2167-2174.
12. S. S. Shinde, A. Maroz, M. P. Hay, A. V. Patterson, W. A. Denny and R. F. Anderson, *J. Am. Chem. Soc.*, 2010, **132**, 2591-2599.
13. J.-T. Hwang, M. M. Greenberg, T. Fuchs and K. S. Gates, *Biochemistry*, 1999, **38**, 14248-14255.
14. V. Junnotula, U. Sarkar, S. Sinha and K. S. Gates, *J. Am. Chem. Soc.*, 2009, **131**, 1015-1024.
15. S. S. Shinde, R. F. Anderson, M. P. Hay, S. A. Gamage and W. A. Denny, *J. Am. Chem. Soc.*, 2004, **126**, 7865-7874.
16. D. Rischin, L. Peters, R. Fisher, A. Macann, J. Denham, M. Poulsen, M. Jackson, L. Kenny, M. Penniment, J. Corry, D. Lamb and B. McClure, *J. Clin. Oncol*., 2005, **23**, 79-87.
17. J. von Pawel, R. von Roemeling, U. Gatzemeier, M. Boyer, L. O. Elisson, P. T. D. Clark, A. Rey, T. W. Butler, V. Hirsh, I. Olver, B. Bergman, J. Ayoub, G. Richardson, D. Dunlop, A. Arcenas, R. Vescio, J. Viallet and J. Treat, *J. Clin. Oncol.*, 2000, **18**, 1351-1359.
18. D. Rischin, L. J. Peters, B. O'Sullivan, J. Giralt, R. Fisher, K. Yuen, A. Trotti, J. Bernier, J. Bourhis, J. Ringash, M. Henke and L. Kenny, *J. Clin. Oncol*., 2010, **28**, 2989-2995.
19. D. Rischin, R. J. Hicks, R. Fisher, D. Binns, J. Corry, S. Porceddu and L. J. Peters, *J. Clin. Oncol.*, 2006, **24**, 2098-2104.
20. L. J. Peters, B. O'Sullivan, J. Giralt, T. J. Fitzgerald, A. Trotti, J. Bernier, J. Bourhis, K. Yuen, R. Fisher and D. Rischin, *J. Clin. Oncol.*, 2010, **28**, 2996-3001.
21. K. O. Hicks, F. B. Pruijn, T. W. Secomb, M. P. Hay, R. Hsu, J. M. Brown, W. A. Denny, M. W. Dewhirst and W. R. Wilson, *J. Natl. Cancer Inst*., 2006, **98**, 1118-1128.
22. M. P. Hay, K. O. Hicks, K. Pchalek, H. H. Lee, A. Blaser, F. B. Pruijn, R. F. Anderson, Shinde, S.S., W. R. Wilson and W. A. Denny, *J. Med. Chem.*, 2008, **51**, 6853-6865.
23. P. Wardman, M. F. Dennis, S. A. Everett, K. B. Patel, M. R. L. Stratford and M. Tracy, *Biochem. Soc. Symp*., 1995, **61**, 171-194.
24. S. S. Shinde, M. P. Hay, A. V. Patterson, W. A. Denny and R. F. Anderson, *J. Am. Chem. Soc.*, 2009, **131**, 14220-14221.
25. H. A. O. Hill and P. J. Thornalley, *Biochim. Biophys. Acta*, 1983, **762**, 44-51.
26. E. G. Janzen, R. V. Shetty and S. M. Kunanec, *Can. J. Chem.*, 1981, **59**, 756-758.
27. O. Augusto, P. R. Ortiz de Montellano and A. Quintanilha, *Biochem. Biophys. Res. Commun.*, 1981, **101**, 1324-1330.
28. M. Birincioglu, P. Jaruga, G. Chowdhury, H. Rodriguez, M. Dizdaroglu and K. S. Gates, *J. Am. Chem. Soc.*, 2003, **125**, 11607-11615.
29. G. Chowdhury, V. Junnotula, J. S. Daniels, M. M. Greenberg and K. S. Gates, *J. Am. Chem. Soc.*, 2007, **129**, 12870-12877.
30. J. S. Daniels and K. S. Gates, *J. Am. Chem. Soc.*, 1996, **118**, 3380-3385.
31. K. Ranguelova and R. P. Mason, *Magn. Reson. Chem*., 2011, **49**, 152-158.
32. K. Stolze, N. Udilova and H. Nohl, *Free Radic. Biol. Med.*, 2000, **29**, 1005-1014.
33. W. T. Dixon, R. O. C. Norman and A. L. Buley, *J. Chem. Soc.*, 1964, 3625-3634.
34. H. Karoui, F. Chalier, J.-P. Finet and P. Tordo, *Org. Biomol. Chem.*, 2011, **9**, 2473-2480.
35. R. E. Krisch, P. M. Tan and M. B. Flick, *Radiat. Res.*, 1985, **101**, 356-372.
36. A. V. Patterson, M. P. Saunders, E. C. Chinje, L. H. Patterson and I. J. Stratford, *Anti-Cancer Drug Design*, 1998, **13**, 541-573.
37. P. L. Olive, *Radiat. Res.*, 1998, **150**, S42-S51.
38. P. Pfeiffer, W. Goedecke and G. Obe, *Mutagenesis*, 2000, **15**, 289-302.
39. J. Griffiths and J. A. Murphy, *J. Chem. Soc. Commun.* 1992, 24-26.
40. K. Hiramoto, M. Kaku, T. Kato and K. Kikugawa, *Chem.-Biol. Interact.*, 1995, **94**, 21-36.
41. M. Boyd, M. P. Hay and P. D. Boyd, *Magn. Reson. Chem.*, 2006, **44**, 948-954.
42. R. F. Anderson, W. A. Denny, W. Li, J. E. Packer, M. Tercel and W. R. Wilson, *J. Phys. Chem.* A, 1997, **101**, 9704-9709.
43. Y. Gu, Patterson, A. V., Atwell, G. J., Chernikova, S. B., Brown, J. M., Thompson, L. H., Wilson, W. R. *Mol. Cancer Ther*., 2009, **8**, 1714-1723.
44. Guise, C. P., Abbattista, M. R., Tipparaju, S. R., Lambie, N. K., Su, J., Li, D., Wilson, W. R., Dachs, G. U. and Patterson, A. V. *Mol. Pharmacol.* 2012, **81**, 31-40.
45. C. H. Williams, Jr. and K. H., *J. Biol. Chem.*, 1962, **237**, 587-595.
46. F. P. Guengerich, M. V. Martin, C. D. Sohl and Q. Cheng, *Nat. Protoc.*, 2009, **4**, 1245-1251.
47. H. A. Schwarz and R. W. Dodson, *J. Phys. Chem.*, 1989, **93**, 409-414.
48. P. Wardman, *J. Phys. Chem. Ref. Data*, 1989, **18**, 1637-1755.
49. M. Jonsson, J. Lind, T. Reitberger, T. E. Eriksen and G. Merenyi, *J. Phys. Chem.*, 1993, **97**, 11278-11282.
50. M. J. Frisch and et al., Revision A, 02ed, 2009, Guassian, Inc.: Wallingford CT.
51. A. D. Becke, *Physical Review A*, 1988, **38**, 3098-3100.
52. A. D. Becke, *J. Chem. Phys.*, 1993, **98**, 5648-5642.
53. C. T. Lee, W. T. Yang and R. G. Parr, *Physical Review B*, 1988, **37**, 785-789.
54. M. J. Frisch, J. A. Pople and J. S. Binkley, *J. Chem. Phys.*, 1984, **80**, 3265-3269.
55. P. C. Hariharan and J. A. Pople, *Theoretica Chim. Acta*, 1973, **28**, 213-222.
56. M. W. Wong, Che. *Phys. Lett.*, 1996, **256**, 391-399.
57. J. Tomasi, B. Mennucci and R. Cammi, *Chem. Rev.*, 2005, **105**, 2999-3093.